

Hard X-ray Emission Associated with White Dwarfs

Ian J. O'Dwyer, You-Hua Chu, Robert A. Gruendl, Martín A. Guerrero, Ronald F.

Webbink

Department of Astronomy, University of Illinois, 1002 W. Green Street, Urbana, IL 61801;

iodwyer@astro.uiuc.edu, chu@astro.uiuc.edu, gruendl@astro.uiuc.edu, mar@astro.uiuc.edu,

webbink@astro.uiuc.edu

Received _____; accepted _____

ABSTRACT

Inspired by the hard X-ray emission from WD 2226–210, the central star of the Helix Nebula, we have made a systematic search for similar sources by correlating the white dwarf catalog of McCook & Sion (1999) and the *ROSAT* PSPC point source catalog of White, Giommi, & Angelini (2000). We find 76 white dwarfs coincident with X-ray sources at a high level of confidence. Among these sources, 17 show significant hard X-ray emission at energies > 0.5 keV. Twelve of these white dwarfs with hard X-ray emission are in known binary systems, in two of which the accretion of the close companion’s material onto the white dwarf produces hard X-ray emission, and in the other ten of which the late-type companions’ coronal activity emits hard X-rays. One apparently single white dwarf is projected near an AGN which is responsible for the hard X-ray emission. The remaining four white dwarfs and two additional white dwarfs with hard X-ray emission appear single. The lack of near-IR excess from the apparently single white dwarfs suggests that either X-ray observations are more effective than near-IR photometry in diagnosing faint companions or a different emission mechanism is needed. It is intriguing that 50% of the six apparently single white dwarfs with hard X-ray emission are among the hottest white dwarfs. We have compared X-ray properties of 11 hot white dwarfs with different spectral types, and conclude that stellar pulsation and fast stellar winds are not likely the origin of the hard X-ray emission, but a leakage of the high-energy Wien tail of emission from deep in the stellar atmosphere remains a tantalizing source of hard X-ray emission from hot DO and DQZO white dwarfs. A complete survey using the entire *ROSAT* PSPC archive is needed to enlarge the sample of white dwarfs with hard X-ray emission. Follow-up near-IR photometric observations are needed to verify the existence of late-type companions and high-resolution

deep X-ray observations are needed to verify the positional coincidence and to study the X-ray spectral properties in order to determine the origin and nature of the hard X-ray emission.

Subject headings: white dwarfs – binaries: general – stars: coronae – stars: late-type – X-rays

1. Introduction

White dwarfs can be sources of soft (< 0.4 keV) X-ray emission if their atmospheres have high temperatures and low opacities: $T_{\text{eff}} \gtrsim 23,000$ K for DA white dwarfs with pure hydrogen atmospheres (Jordan et al. 1994), $23,000$ K $\lesssim T_{\text{eff}} \lesssim 54,000$ K for DA white dwarfs containing significant quantities of heavy elements in their atmospheres (Marsh et al. 1997), and $T_{\text{eff}} \gtrsim 100,000$ K for DO and PG 1159 white dwarfs with helium-rich atmospheres (Motch, Werner, & Pakull 1993). *ROSAT* observations of such X-ray sources show soft spectra rising toward *ROSAT*'s low-energy limit at 0.1 keV. The DO white dwarf KPD 0005+5106 (= WD 0005+511), with its spectrum peaking at 0.2 keV, appears to pose an exception and has been interpreted as having cool ($2 - 3 \times 10^5$ K) coronal emission (Fleming, Werner, & Barstow 1993). *No hard X-ray (> 0.5 keV) emission is expected from single white dwarfs.*

It is thus puzzling that WD 2226–210¹, the 103,600 K DAO white dwarf (Méndez et al. 1988; Napiwotzki 1999) in the Helix Nebula, appears to be single (Ciardullo et al. 1999), but has hard X-ray emission. *ROSAT* observations of WD 2226–210 have detected not only a soft spectral component as expected from the white dwarf's photosphere, but also a hard

¹This white dwarf was cataloged with a sign error in declination as WD 2226+210 by McCook & Sion (1999).

spectral component peaking at 0.8 keV (Leahy, Zhang, & Kwok 1994). Recent *Chandra* observations have confirmed that the hard X-ray emission is unresolved and coincident with the white dwarf; however, the luminosity and variability of the hard X-ray emission is similar to that of a dMe star (Guerrero et al. 2001). Follow-up spectroscopic observations by Gruendl et al. (2001) detected variability in the H α line profile of WD 2226–210, suggesting the presence of a companion. It is thus possible that WD 2226–210 has an X-ray-emitting dMe companion which is too faint and close to the white dwarf to be detected at visible wavelengths. Based on the *I* magnitude of WD 2226–210 reported by Ciardullo et al. (1999) and the *J*, *H*, and *K* magnitudes from the 2MASS Survey (see Table 3 below), we estimate that the hypothetical companion must have a spectral type later than M5–6 V.

Hard X-ray emission from white dwarfs may be used to infer the presence of a binary companion. Indeed, Fleming et al. (1996) found 9 DA white dwarfs with hard X-ray emission using the *ROSAT* All-Sky Survey, and all of these 9 white dwarfs have late-type (F, G, K, and M) companions. This has motivated us to search for other white dwarfs which exhibit hard X-ray emission. We have found that 94 white dwarfs cataloged by McCook & Sion (1999) appear coincident with *ROSAT* X-ray point sources in the WGA catalog (White, Giommi, & Angelini 2000, hereafter WGACAT). To confirm the positional coincidence, we have downloaded the *ROSAT* data, and compared these X-ray images with optical images of the white dwarfs. We have further extracted the *ROSAT* spectra to examine whether hard X-ray emission is present. For white dwarfs associated with hard X-ray emission, we have used the literature and near-IR photometry to assess the existence of binary companions, and further investigate the origin of hard X-ray emission from the apparently single white dwarfs. This paper reports the results of our study. The sample of white dwarfs with hard X-ray emission and our method of analysis are described in Section 2, the binarity status of the white dwarfs with hard X-ray emission is reported in Section 3, and the origin and implications of the hard X-ray emission associated with white dwarfs is

discussed in Section 4. A summary is given in Section 5.

2. Search for Hard X-ray Sources Associated with White Dwarfs

To search for X-ray emission from white dwarfs, we have correlated the white dwarfs from the most recent catalog by McCook & Sion (1999) with the X-ray sources from the WGACAT, a point source catalog generated from all *ROSAT* PSPC pointed observations made without the boron filter. For an initial identification of positional coincidence, we require better than $1'$ agreement between the cataloged positions of the white dwarf and X-ray point source. This is a conservative criterion because: (1) the on-axis point spread function (PSF) of the *ROSAT* Position Sensitive Proportional Counter (PSPC) is $\sim 40''$ at 1 keV and much worse near 0.1 keV (Snowden et al. 1994; Chu, Kwitter, & Kaler 1993), (2) the coordinates of the white dwarf might be uncertain by up to $30''$, and (3) the proper motions of the white dwarfs have not been considered and in some cases may be large enough for the star to move more than $1'$ between the epochs when the optical and X-ray observations were made.

We find 94 white dwarfs that appear to be associated with point X-ray sources. To confirm the positional coincidence and to examine further the X-ray spectra of these sources, we have retrieved the event files of their *ROSAT* PSPC observations from the High Energy Astrophysics Science Archive Research Center (HEASARC) at NASA's Goddard Space Flight Center. The PSPC event files are used to extract broad-band (0.1–2.4 keV) X-ray images. These X-ray images are smoothed with a Gaussian with $\sigma = 15''$ and the resulting X-ray contours at 10, 20, 50, 70, and 90% of the peak intensity are overplotted on the broad-band optical images retrieved from the Digitized Sky Survey (DSS). To identify the white dwarfs, we have used the finding charts provided by J. Holberg at <http://procyon.lpl.arizona.edu/WD/>.

The results of our detailed comparison of the positions of X-ray sources and white dwarfs are presented in Table 1. Columns 1–3 give the identifications, common names, and spectral types of the white dwarfs; columns 4–6 list the corresponding X-ray sources in the WGACAT, the *ROSAT* PSPC observations used for the detection, and the exposure times of the PSPC observations; column 7 describes the positional coincidence between the X-ray source and the white dwarf; and columns 8–10 present the counts detected in the soft (0.1–0.4 keV), medium (0.4–0.9 keV), and hard (0.9–2.0 keV) bands, as reported in the WGACAT.

Eighteen of the 94 coincidences we initially identified could not be confirmed, noted as U1–4 in column 7 of Table 1, because the X-ray sources are not convincingly centered on the white dwarf (U1), the positions of the X-ray sources are compromised by the occultation of the PSPC window support structure or the superposition of a bright background (U2), multiple candidates of optical counterparts are present within the PSPC PSF (U3), or the X-ray sources are too faint to be credible (U4).

One notable example of a U4 mis-identification is WD 1910+047, which was discovered and suggested by Margon, Bolte, & Anderson (1987) to be associated with an *Einstein* X-ray source. The weak WGACAT source J1912.5+0452 located within 1' from WD 1910+047 was detected in a 2.8 ks PSPC observation (rp400271n00) at a 44' off-axis position, but not confirmed in a 20 ks PSPC observation (rp400271a01) with identical pointing. We have examined this shallow PSPC observation and concluded that this source is spurious. Using a deep PSPC observation (rp500058a02, 20.6 ks) centered at 19' from WD 1910+047, we find an X-ray source near the white dwarf, but it is coincident with a star $\sim 80''$ SE of the white dwarf and the X-ray spectrum is typical for coronal emission from a late-type star (see Figure 1). This result explains the conclusion of the model atmosphere analysis by Vennes (1990) that the *Einstein* X-ray source is too luminous for the white dwarf.

There remain 76 coincidences that are confirmed with a high degree of confidence. We have further extracted X-ray spectra from the PSPC event files for these X-ray sources coincident with white dwarfs. We find 69 dominated by soft X-ray emission (<0.5 keV), as expected from white dwarfs; however, 10 of these also exhibit hard X-ray emission (0.5–2.4 keV). The spectra of the remaining 7 sources have characteristics consistent with coronal emission at temperatures of a few $\times 10^6$ K. These PSPC spectra appear “double-peaked” because of the carbon $K\alpha$ absorption of the PSPC entrance window at 0.24–0.4 keV; the hard component (>0.5 keV) is at least 25% as strong as the soft component (<0.5 keV).

The 17 white dwarfs associated with hard X-ray emission are listed in Table 2, and their images and X-ray spectra are presented in Figure 2. The left panels display DSS images centered on the white dwarfs and overlaid by X-ray contours to illustrate the positional coincidence of the white dwarf and the X-ray source. The white dwarf position is marked when several stars are projected in its vicinity. The right panels display the PSPC spectra of the X-ray sources. For objects overwhelmed by soft X-ray emission, we also plot the spectra with an expanded Y-scale to show the hard component. The PSPC observations listed in Table 1 have been used to extract these X-ray images and spectral information.

Note that Column 10 of Table 1 shows many more white dwarfs with 3σ detections in the 0.9–2.4 keV band. However, all except the above 17 white dwarfs are rejected because their coincidences with X-ray source are not confirmed (U1-4 in Column 7) or the WGACAT source counts are contaminated/confused with background hard X-ray sources. For example, some white dwarfs are observed at such large off-axis angles ($> 40'$) that the PSF contains background sources (e.g., WD 0037+312 and WD 1040+451), and some are blended with adjacent sources (e.g., WD 1821+643, WD 1844–654, and WD 0904+511). Under such circumstances, the source detection algorithm of WGACAT does not effectively exclude contaminating background sources within the PSF, resulting in the apparent

detection of hard X-ray emission.

3. Binarity of White Dwarfs with Hard X-ray Emission

White dwarfs by themselves do not emit hard (> 0.5 keV) X-rays. If a white dwarf accretes material from its surroundings, the gravitational energy released may power hard X-ray emission. In general, we can rule out the accretion of interstellar material because white dwarfs usually are not in a dense interstellar environment. We can also rule out the accretion of the planetary nebula produced by a white dwarf’s progenitor, as it either has dissipated already or is expanding away at a speed much greater than the escape velocity. Thus, the most likely source to provide material for accretion onto a white dwarf is a binary companion. Alternatively, if a white dwarf has a binary companion with coronal activity, the hard X-ray emission from the companion would appear to be associated with the white dwarf. We therefore suspect that white dwarfs with hard X-ray emission are in binary systems.

A literature search of the 17 white dwarfs with hard X-ray emission reveals that 12 of them are known binaries. Below we describe these 12 known binary systems in §3.1, and the 5 apparently single white dwarfs in §3.2.

3.1. Known Binaries

WD 0216–032 (VZ Cet) is a detached companion of Mira, a pulsating, cool giant (M2-7 III). Karovska et al. (1997) measured a separation and position angle $\rho = 0''.578$, $\theta = 108.3^\circ$ (Ep. 1995.9424). Baize (1980) estimated an orbital period of 400 yr for this system (separation $a = 0''.85$), but this result is extremely uncertain (Mason et al. 2001). The white dwarf flickers (Warner 1972), and *IUE* observations suggest that it may possess

an accretion disk (Reimers & Cassatella 1985). The PSPC spectrum shows X-ray emission peaking at 1 keV. This hard X-ray emission probably originates from the accretion, since no single cool giants similar to Mira are known X-ray sources.

WD 0347+171 (V471 Tau) is in the eclipsing binary system V471 Tau with a period of 0.521 days (Nelson & Young 1970; Guinan & Sion 1984). The K2 V companion is known for its coronal activity, and coronal mass ejections have been implied from the observations of transient absorption features in the Si III λ 1206 resonance line (Bond et al. 2001). Using X-ray and EUV eclipses of V471 Tau, Barstow et al. (1992) have demonstrated that the hard X-ray emission indeed originates from the K2 V star.

WD 0429+176 (HZ 9) is in a spectroscopic binary system with a dM4.5e companion and a period of 0.564 days (Lanning & Pesch 1981; Guinan & Sion 1984). Late-type main sequence M stars, particularly the ones with Balmer lines in emission (i.e., dMe stars), have been shown to be X-ray emitters (Rucinski 1984). The dM4.5e companion of WD 0429+176 is most likely responsible for the hard X-ray emission detected.

WD 0736+053 (Procyon B) is a visual binary companion of Procyon A, an F5 IV-V star, with a period of 40.8 yr (Girard et al. 2000). The coronal activity of Procyon A is responsible for the hard X-ray emission (Lemen et al. 1989). In Figure 2, the wavy line shows the motion (proper and orbital) of the white dwarf between the epochs of DSS and *ROSAT* PSPC observations.

WD 1213+528 (EG UMa) was observed at a large off-axis angle. The PSPC PSF extends over almost $2'$, but the white dwarf appears to be the most likely optical counterpart of the X-ray source. WD 1213+528 has a dM2e binary companion in a 0.668 day period (Lanning 1982).

WD 1255+258J (HD 112313B) is the central star of the planetary nebula LoTr 5, and

has a G5 III companion with a rotational period of 5.9 days (Jasniewicz et al. 1996). The orbital period of this binary is unknown, but probably in excess of one year; the binary is unresolved. The strong Ca II H & K emission lines and broad variable H α line of the G5 III companion suggest coronal activity. Thus the G5 III companion is probably responsible for the observed hard X-ray emission.

WD 1314+293 (HZ 43A) has a dM3.5e companion (Napiwotzki et al. 1993), resolved at $\rho = 2''.2$, $\theta = 263^\circ$ (Ep. 1996; Mason et al. 2001). This companion is likely responsible for the hard X-ray emission detected.

WD 1631+781 (1ES 1631+78.1) has an unresolved dM4e companion (Catalan et al. 1995). From the lack of detectable radial velocity variations (Sion et al. 1995), we conclude that the orbital period probably exceeds one year. Fluctuations in H β emission from the dM4e companion mark it as the probable site of hard X-ray emission.

WD 1633+572 (GJ 630.1B) is the common proper motion companion ($\rho = 26''.19$, $\theta = 22.46^\circ$ at Ep. 2000.0 from an astrometric fit to six DSS plates) of the variable star CM Dra (Greenstein 1986). CM Dra is itself an eclipsing binary containing two dM3-4e stars with a period of 1.26 days (Lacy 1977). The proper motion of CM Dra is so large that it must be considered when comparing the DSS and *ROSAT* PSPC images. In Figure 2, we have drawn an arrow to show the proper motion of CM Dra between the optical and X-ray epochs. The X-ray source is centered on CM Dra, rather than the white dwarf; therefore, the hard X-ray emission clearly originates from the dM3-4e binary.

WD 1634–573 (HD 149499B) is in a wide binary system ($\rho = 1''.319$, $\theta = 51.71^\circ$ at Ep. 1991.25, from Hipparcos) with a K2 Ve companion (Wegner 1979, 1981). The emission lines in the companion’s spectrum are indicative of coronal activity, which may be responsible for the hard X-ray emission.

WD 1944–421 (V3885 Sgr) is a cataclysmic variable with orbital period 0.216 days (Downes et al. 2001). Among our sample of 17 white dwarfs with hard X-rays, this is the only one whose hard X-ray component is stronger than the soft X-ray component, indicating a different emission mechanism. The X-ray emission from WD 1944–421 must originate from the accretion of material from a binary companion onto the surface of the white dwarf (Patterson 1994).

WD 2154–512 (GJ 841B) is a visual companion of GJ 841A ($\rho = 27''.93$, $\theta = 251.5^\circ$, Ep. 1987.23, from measurements on 2 DSS plates), which consists of two chromospherically active dM3–5e stars with an orbital period of 1.124 days (Jeffries & Bromage 1993). The dMe stars in GJ 841A are most likely responsible for the hard X-ray emission detected.

3.2. The Apparently Single White Dwarfs

WD 0339–451 has an X-ray spectrum similar to those associated with stellar coronal emission. The temperature of this DA white dwarf is unknown, but its photospheric emission probably does not contribute much to the X-ray emission detected since the spectrum below 0.5 keV does not rise toward 0.1 keV as expected.

WD 1134+300 (GJ 433.1) is a DA2 white dwarf that has been used as a spectrophotometric standard star (Massey & Gronwall 1990; Hawarden et al. 2001). Its PSPC spectrum shows a distinct peak at 0.8–0.9 keV. Detailed inspection shows that the soft X-ray emission is centered at the white dwarf, but the hard X-ray emission is centered at a position $\sim 41''$ northwest of the white dwarf, where an AGN has been identified by Mason et al. (2000). This background AGN must be responsible for the hard X-ray emission.

WD 1159–034 (GW Vir), the prototype of PG 1159 white dwarfs, is a well-known pulsating variable (Winget, Hansen, & van Horn 1983). The faint hard X-ray emission is

centered on the white dwarf, but the spectrum is too noisy for detailed spectral analysis.

WD 1234+481 (PG 1234+481) does not have X-ray emission peaking at ~ 0.9 keV as the other white dwarfs associated with hard X-ray emission do. However, the spectrum of WD 1234+481 appears to show excess emission at 0.4–0.6 keV.

WD 1333+510 (PG 1333+510) is detected at a large off-axis angle, but it is the closest source, among three, to the peak of the X-ray emission. The X-ray spectrum is similar to those of stellar coronae.

4. Discussion

X-ray emission from white dwarfs is expected to be soft, but roughly 20% of X-ray sources associated with white dwarfs exhibit a hard X-ray component (>0.5 keV). What is the origin of hard X-ray emission associated with white dwarfs? We initially speculated that all white dwarfs with hard X-ray emission possess binary companions, but our literature search reveals that 12 of the 17 white dwarfs with hard X-ray emission are known to be in binary or multiple systems, one is superposed by chance near a background AGN, and the remaining four are apparently single white dwarfs. Below we argue that the binary companions are indeed directly or indirectly responsible for the hard X-ray emission associated with white dwarfs in binary systems, use 2MASS photometry to assess the existence of late-type companions, and discuss the hard X-ray emission from the hottest apparently single white dwarfs.

4.1. Hard X-ray Emission Associated with White Dwarfs in Binary Systems

Two of our 12 white dwarfs in binary systems are known to accrete material from their companions: Mira and the cataclysmic variable V3885 Sgr. The accretion of the companion’s material onto the surface of the white dwarf produces hard X-ray emission (Patterson 1994). Of the ten non-accreting systems, six have one or two dMe companions, two have a K2V companion, one has an F5IV-V companion, and one has a G5III companion. These late-type companions either are known for their active coronae or have emission lines indicating coronal activity; therefore, these companions are most likely responsible for the observed hard X-ray emission. In some cases, the origin of the hard X-ray emission has been unambiguously established to be the late-type companions by either positional coincidence (e.g., WD 1633+572) or observations of eclipses (e.g., WD 0347+171).

To confirm that these late-type companions are the source of the hard X-ray emission, we compare the hard X-ray luminosities and plasma temperatures of the binary systems with those expected from single late-type stars. We have fitted thin plasma emission models (Raymond & Smith 1977) to the 0.5–2.4 keV portion of the spectra for the objects with sufficient counts in this energy band. The resultant plasma temperature kT and X-ray luminosity L_X in the 0.5–2.4 keV band are given in Table 2. The L_X of white dwarfs with late-type companions are completely consistent with those seen in dM and K stars, 10^{27} – 10^{29} ergs s⁻¹ (Schmitt, Fleming, & Giampapa 1995; Marino, Micela, & Peres 2000). The best-fit plasma temperatures are also in the range for stellar coronae. We further assess whether coronal activities of the late-type companions may be induced by binary interaction by correlating the projected binary separation, a , with the X-ray luminosity (see Table 2). No clear correlation is seen. This lack of correlation may be caused by the small number of binary systems in our sample and the wide range of physical parameters involved. The cataclysmic variable WD 1944–421 (V3885 Sgr) has the highest hard X-ray

luminosity, which is also in accord with the expectation of accretion from a Roche-lobe-filled companion. Thus, the hard X-ray emission from white dwarfs in known binary systems can be explained by the presence of their companions.

4.2. Apparently Single White Dwarfs

The remaining four white dwarfs associated with hard X-ray emission appear to be single. If these white dwarfs contain previously-unknown, late-type companions, near-IR photometry may reveal these companions (e.g., Green, Ali, & Napiwotzki 2000). We have obtained *JHK* photometric measurements of white dwarfs with hard X-rays available in the second incremental data release of the Two Micron All Sky Survey (2MASS), and listed them in Table 3, along with optical photometry from McCook & Sion (1999). In the case of WD 1633+572 where the white dwarf and the binary dMe companions are resolved by 2MASS, separate entries are given. To enlarge the sample for comparison, we have added two additional white dwarfs with hard X-ray emission that are not from our survey: WD 0005+511 (= KPD 0005+5106; its hard X-ray emission will be discussed in §4.3) and WD 2226–210 (= the central star of the Helix Nebula; its hard X-ray emission is described in §1).

Clear near-IR excess is observed in the four known binary systems, but not in the apparently single white dwarfs. The lack of near-IR excess, in conjunction with known distances, places constraints on the possible companions of the white dwarfs. The constraint is more stringent for white dwarfs at smaller distances because it would be harder to hide a companion. The nearest apparently single white dwarf with hard X-ray emission is WD 1134+300 at 15.3 pc. We estimate that its near-IR magnitudes can hide only a brown dwarf companion more than 3 mag fainter than an M7 V star. Therefore, WD 1134+300 has no stellar-mass companions, and the AGN projected within the PSPC PSF (Mason et

al. 2000) is solely responsible for the hard X-ray emission observed.

Two other white dwarfs with hard X-ray emission have known distances, WD 1234+481 and WD 2226–210. Their lack of near-IR excess indicates that WD 1234+481 can hide a companion of spectral type M7 V or later, and WD 2226–210 later than M5-6 V. If these two apparently single white dwarfs indeed have faint, late-type companions, then the hard X-ray emission detected by *ROSAT* is more effective than the near-IR excess detected by 2MASS in diagnosing the existence of a faint late-type companion.

4.3. Hard X-ray Emission from the Hottest Apparently Single White Dwarfs

Two of the apparently single white dwarfs associated with hard X-rays from our survey are among the hottest known: WD 1159–034 and WD 2226–210. To compare these two hot white dwarfs to the one that has been suggested to possess a corona, KPD 0005+5106, we have retrieved an archival *ROSAT* PSPC pointed observation (rf200428n00) that was made with the boron filter for an exposure time of 5 ks. As shown in Figure 3, the PSPC spectrum of KPD 0005+5106 shows not only the soft atmospheric emission below 0.5 keV, but also hard X-ray emission near 1 keV. This hard X-ray emission was not detected previously by Fleming, Werner, & Barstow (1993) using the *ROSAT* All-Sky Survey observation of exposure time 504 s. As the 5 ks pointed observation detected only 24 ± 6 counts in the 0.5–2.4 keV band, if the hard X-ray flux is constant, we expect only 2.4 ± 1.5 hard X-ray counts in a 504 s exposure. The non-detection of the hard component by Fleming, Werner, & Barstow (1993) thus does not imply a temporal variation. The presence of hard X-ray emission from KPD 0005+5106 requires a plasma temperature at least 10^6 K, much higher than that suggested by Fleming, Werner, & Barstow (1993), and may be responsible for photoionizing O VIII and producing the recombination lines observed (Werner & Heber 1992; Sion & Downes 1992). We have examined the 2MASS

JHK photometric data for KPD 0005+5106 (see Table 3), and find no evidence for a near-IR excess. Thus, KPD 0005+5106 is another apparently single hot white dwarf with hard X-ray emission.

While our statistical sample is extremely limited, it is intriguing that $\sim 50\%$ of the apparently single white dwarfs with hard X-ray emission are among the hottest known white dwarfs: 120,000 K for WD 0005+511 (=KPD 0005+5106; Werner, Heber, & Fleming 1994), 140,000 K for WD 1159–034 (= PG 1159–034; Dreizler & Heber 1998), and 103,600 K for WD 2226–210 (= CSPN of the Helix; Napiwotzki 1999). Is it possible that the hard X-ray emission is the high-energy Wien tail of the blackbody emission from deep in the stellar atmosphere? It is beyond the scope of this paper to model the atmospheres of these white dwarfs and answer this question theoretically. Instead, we will examine X-ray observations of the hottest white dwarfs to search for trends in their hard X-ray properties in order to gain insight into the origin of their hard X-ray emission.

We first examine X-ray properties of PG 1159 stars. Many pointed *ROSAT* PSPC observations of PG 1159 stars were made with the boron filter. These X-ray sources will be absent in the WGACAT, and it is necessary to search the *ROSAT* archive for pointed and serendipitous observations of PG 1159 stars. PG 1159 stars are divided into two groups: with and without planetary nebulae (PNs). *ROSAT* observations of cataloged PNs have been analyzed and reported by Guerrero, Chu, & Gruendl (2000); PSPC observations of five PNs with PG 1159 central stars are available. Of these five, WD 0726+133 (in Abell 21; PG 1159) and WD 2333+301 (in Jn 1; DOZ.3) are not detected; WD 2117+342J (in MWP 1; DO) is detected at a 40' off-axis position in the PSPC field-of-view (this paper), but the poor PSF does not allow us to assess accurately whether faint hard X-ray emission exists; WD 0044–121 (in NGC 246; PG 1159) and WD 1821+643 (in K 1-16; DOZ.4) are centered in pointed PSPC observations, but only soft (<0.5 keV) X-ray emission from the

white dwarf is detected. Four PG 1159 stars without PNs have pointed PSPC observations: WD 0122–753J (= RX J0122–7521; DO), WD 1144+004 (= PG 1144+005; DQZO1), WD 1159–034 (= PG 1159–034; DQZO.4), and WD 1501+664 (= PG 1501+661; DZ1); all four have been included in our survey listed in Table 1. Soft X-ray emission is detected in these four PG 1159 stars without PNs, but $3\text{-}\sigma$ detection of hard X-rays is obtained only for PG 1159 itself.

We have further combed Table 1 for hot white dwarfs similar to WD 0005+511 or WD 2226–210, and find a hot DO white dwarf, WD 1522+662, and a hot DAO white dwarf, WD 1957+225 at the center of the Dumbbell Nebula. These four hot DO and DAO white dwarfs and the above nine PG 1159 white dwarfs will be discuss below in more detail. The spectral type, stellar effective temperature, visual magnitude, and *ROSAT* observations of these 13 hot white dwarfs are summarized in Table 4. To illustrate the spectral properties of the 11 hot white dwarfs whose X-ray emission has been detected by *ROSAT* PSPC observations, in Figure 4 we present their soft X-ray images in the 0.1–0.4 keV band and the hard X-ray images in the 0.6–2.4 keV band. It is evident that hard X-ray emission is clearly detected only from WD 0005+511, WD 1159–034, and WD 2226–210, as we have concluded earlier, and possibly detected at a 2σ level from WD 0122–753J. The spectral types of these four white dwarfs are DO, DQZO.4, DAO, and DO, respectively.

Below we divide the 11 hot white dwarfs detected in X-rays according to their spectral types, discuss the implications of their hard X-ray properties, and speculate on the possibility of a photospheric origin of the hard X-ray emission.

- *DAO (WD 1957+225 and WD 2226–210):*

Hard X-ray emission is detected from WD 2226–210 in the Helix Nebula, but not from WD 1957+225 in the Dumbbell Nebula. As these two DAO white dwarfs have similar effective temperatures, and as WD 1957+225 is only 0.8 mag fainter but has a

four times longer exposure time, the lack of hard X-ray emission from WD 1957+225 signifies a real difference from WD 2226–210. Furthermore, WD 2226–210 shows temporal variations of its hard X-ray emission and H α line profile, suggesting the existence of a late dMe companion (Guerrero et al. 2001; Gruendl et al. 2001). Therefore, there is no evidence indicating that deep photospheric emission is the origin of hard X-rays associated with DAO white dwarfs.

- *DO (WD 0005+511, WD 0122–753J, WD 1522+662, and WD 2117+342J):*

Among these four DO white dwarfs, WD 0005+511 has an unambiguous detection of hard X-rays, and WD 0122–753J has a possible detection of hard X-rays.

WD 1522+662 does not show hard X-ray emission, but the *ROSAT* observation has only 4.7 ks exposure time and WD 1522+662 is faint with $B = 16.4$ mag.

WD 2117+342J is observed at a 40' from the center of the PSPC field-of-view and the poor PSF prohibits a conclusive assessment of the existence of faint hard X-ray emission. It may be possible that faint hard X-ray emission can emerge from the hot, deep layer of the photospheres of DO white dwarfs, but more detections are needed to confirm it.

- *DQZO (WD 1144+044, WD 1159–034, and WD 1821+643):*

WD 1159–034 has hard X-ray emission. WD 1144+044 has a non-detection, but it is slightly fainter than WD 1159–034 and its exposure time is only half as long.

WD 1821+643 in the PN K 1-16 is projected near a bright hard X-ray source, a cluster of galaxies surrounding the QSO E1821+643 (Saxton et al. 1997), so it is difficult to determine its hard X-ray properties accurately from Figure 4. We have examined an archival *Chandra* HETG observation of QSO E1821+643 (PI: C. R. Canizares; 101 ks); in this observation WD 1821+643 is detected and clearly resolved from QSO E1821+643, but no hard X-ray emission from WD 1821+643 is seen.

WD 1159–034 and WD 1821+643 are well-known pulsators (Ciardullo & Bond 1996), while WD 1144+044 is not. It is thus unlikely that the hard X-ray emission is related to the stellar pulsation.

- *PG 1159 and DZ1 (WD 0044–121 and WD 1501+664):*

WD 0044–121 is a PG 1159 star in the PN NGC 246; WD 1501+664 is classified as DZ1 and is the hottest white dwarf (Werner & Wolff 1999). Neither of these two hot white dwarfs show hard X-ray emission; the high opacity of the H- and He-free atmosphere of WD 1501+664 may be the culprit of its non-detection (Nousek et al. 1986; Werner 1991).

The above sample of hot white dwarfs is very limited, but allows us to eliminate improbable origins of hard X-ray emission. For example, stellar pulsation is not likely to produce hard X-ray emission, as WD 1159–034 is the only pulsator with hard X-ray emission. Stellar winds are not likely to be the origin of hard X-ray emission either, as WD 1159–034 has hard X-rays but no measurable past or ongoing mass loss (Fritz, Leckenby, & Sion 1990), while appreciable mass loss but no hard X-ray emission has been detected from WD 0044–121 and WD 1821+643 (Koesterke & Werner 1998). There leaves the tantalizing suggestion that hard X-rays may be emitted by hot DO and DQZO white dwarfs. While it is necessary to model their atmospheres to understand theoretically whether hard X-rays from beneath the atmosphere may leak through, it is also necessary to obtain better high-resolution X-ray images to confirm that the hard X-ray emission is indeed associated with the white dwarfs (as opposed to background objects projected in their vicinity) and high-quality X-ray spectra for detailed spectral analysis.

5. Summary

We have correlated the recent white dwarf catalog by McCook & Sion (1999) with the *ROSAT* PSPC point source catalog (WGACAT), and found 76 white dwarfs coincident with X-ray sources at a high level of confidence. We have further found that 17 of these sources show hard X-ray emission (> 0.5 keV). Two of these white dwarfs with hard X-ray emission accrete material from their companions, while the other ten have late-type companions that are known to have active coronae and emit hard X-rays. One white dwarf has an AGN projected within the PSPC PSF contributing to the hard X-ray emission. The remaining four white dwarfs (WD 0339–451, WD 1159–034, WD 1234+481, and WD 1333+510) and two additional white dwarfs (WD 0005+511 and WD 2226–210) with hard X-ray emission appear single. The lack of near-IR excess for WD 1234+481 and WD 2226–210 at known distances constrains the possible spectral types of the hidden companions to later than M7 V and M5–6 V, respectively. We suggest that hard X-ray emission may be more effective than near-IR photometry in diagnosing faint, late-type companions of white dwarfs, if the hard X-ray emission associated with the six apparently single white dwarfs indeed originates from hidden companions.

It is intriguing that three of the six apparently single white dwarfs with hard X-ray emission have high stellar effective temperatures. We have searched the *ROSAT* archive for observations of PG 1159 stars and examined the X-ray properties of a sample of 13 hot white dwarfs with different spectral types. Comparisons among these hot white dwarfs lead to the following conclusions: (1) DAO WD 2226–210 most likely possesses a late dMe companion which emits hard X-rays, (2) stellar pulsation cannot be connected to the hard X-ray emission, (3) fast stellar winds are not likely to be the origin of hard X-ray emission, and (4) the high-energy Wien tail of emission deep in the atmospheres of hot DO and DQZO white dwarfs remains a tantalizing explanation for the hard X-ray emission observed.

Our statistics are limited by the incompleteness of the WGACAT, which has been derived solely from pointed *ROSAT* PSPC observations made without filters, while many PSPC observations of white dwarfs were made with a boron filter. A complete survey for white dwarfs with hard X-ray emission using the entire *ROSAT* archive is needed to enlarge the sample. Follow-up high-resolution deep X-ray observations with *Chandra* or *XMM-Newton* are needed to confirm the positional coincidence of the white dwarfs and the X-ray sources, and to study the spectral properties in order to investigate the origin and nature of hard X-ray emission associated with white dwarfs.

We thank the anonymous referee for making critical comments which helped improve our paper. We also thank J. Liebert, R. Napiwotzki, R. Petre, and K. Werner for reading the manuscript and making useful suggestions. This research has made use of the SIMBAD database, operated at CDS, Strasbourg, France, and the Digital Sky Survey produced at the Space Telescope Science Institute under U.S. Government grant NAG W-2166. We have also used data product from the 2MASS, which is a joint project of the University Massachusetts and the Infrared Processing and Analysis Center/California Institute of Technology, funded by NASA and NSF.

REFERENCES

- Baize, P. 1980, *A&AS*, 39, 86
- Barstow, M. A., et al. 1992, *MNRAS*, 255, 369
- Bond, H. E., Mullan, D. J., O’Brien, M. S., & Sion, E. M. 2001, *ApJ*, 560, 919
- Catalan, M. S., Sarna, M. J., Jomaron, C. M., & Connon Smith, R. 1995, *MNRAS*, 275, 153
- Catchpole, R. W., Robertson, B. S. C., Lloyd Evans, T. H. H., Feast, M. W., Glass, I. S., & Carter, B. S. 1979, *SAAO Circ.*, 1, 61
- Chu, Y.-H., Kwitter, K. B., & Kaler, J. B. 1993, *AJ*, 106, 650
- Ciardullo, R., & Bond, H. E. 1996, *AJ*, 111, 2332
- Ciardullo, R., Bond, H. E., Sipior, M. S., Fullton, L. K., Zhang, C.-Y., & Schaefer, K. G. 1999, *AJ*, 118, 488.
- Dahn, C. C., et al. 1982, *AJ*, 87, 419
- Downes, R. A., Webbink, R. F., Shara, M. M., Ritter, H., Kolb, U., & Duerbeck, H. W. 2001, *PASP*, 113, 764
- Dreizler, S. & Heber, U. 1998, *A&A*, 334, 618
- Fleming, T. A., Snowden, S. L., Pfeffermann, E., Briel, U., & Greiner, J. 1996, *A&A*, 316, 147
- Fleming, T. A., Werner, K., & Barstow, M. A. 1993, *ApJ*, 416, L79
- Fritz, M. L., Leckenby, H. J., & Sion, E. M. 1990, *AJ*, 99, 908

- Girard, T. M. et al. 2000, *AJ*, 119, 2428
- Green, P. J., Ali, B., & Napiwotzki, R. 2000, *ApJ*, 540, 992
- Greenstein, J. L. 1986, *AJ*, 92, 859
- Gruendl, R. A., Chu, Y.-H., O'Dwyer, I. J., & Guerrero, M. A. 2001, *AJ*, 122, 308
- Guerrero, M. A., Chu, Y.-H., & Gruendl, R. A. 2000, *ApJS*, 129, 295
- Guerrero, M. A., Chu, Y.-H., Gruendl, R. A., Williams, R. M., & Kaler, J. B. 2001, *ApJ*, 553, L55 [Erratum: *ApJ*, 554, L235]
- Guinan, E. F., & Sion, E. M. 1984, *AJ*, 89, 1252
- Harrington, R. S. & Dahn, C. C. 1980, *AJ*, 85, 454
- Harris, H. C., Dahn, C. C., Monet, D. G., & Pier, J. R. 1997, in *Planetary Nebulae*, IAU Symp. No. 180, ed. H. J. Habing & H. J. G. L. M. Lamers (Dordrecht: Kluwer), p. 40
- Hawarden, T. G., Leggett, S. K., Letawsky, M. B., Ballantyne, D. R., & Casali, M. M. 2001, *MNRAS*, 325, 563
- Hutchings, J. B., Crampton, D., Cowley, A. P., Schmidtke, P. C., McGrath, T. K., & Chu, Y.-H. 1995, *PASP*, 107, 931
- Jasniewicz, G., Thevenin, F., Monier, R., & Skiff, B. A. 1996, *A&A*, 307, 200
- Jeffries, R. D., & Bromage, G. E. 1993, *MNRAS*, 260, 132
- Jordan, S., Wolff, B., Koester, D., & Napiwotzki, R. 1994, *A&A*, 290, 834
- Karovska, M., Hack, W., Raymond, J., & Guinan, E. 1997, *ApJ*, 482, L175

- Koesterke, L., Dreizler, S., & Rauch, T. 1998, *A&A*, 330, 1041
- Koesterke, L., & Werner, K. 1998, *ApJ*, 500, L55
- Lacy, C. H. 1977, *ApJ*, 218, 444
- Lanning, H. H. 1982, *ApJ*, 253, 752
- Lanning, H. H., & Pesch, P. 1981, *ApJ*, 244, 280
- Leahy, D. A., Zhang, C. Y., & Kwok, S. 1994, *ApJ*, 422, 205
- Lemen, J. R., Mewe, R., Schrijver, C. J., & Fludra, A. 1989, *ApJ*, 341, 474
- Margon, B., Bolte, M., & Anderson, S. F. 1987, *AJ*, 93, 1229
- Marino, A., Micela, G., & Peres, G. 2000, *A&A*, 353, 177
- Marsh, M. C., et al. 1997, *MNRAS*, 287, 705
- Mason, K. O. et al. 2000, *MNRAS*, 311, 456
- Mason, B. D., Wycoff, G. L., Hartkopf, W. I., Douglas, G. G., & Worley, C. E. 2001,
The Washington Visual Double Star Catalog, 2001.0 (Washington, DC: US Naval
Observatory)
- Massey, P., & Gronwall, C. 1990, *ApJ*, 358, 344
- McCook, G. P. & Sion, E. M. 1999, *ApJS*, 121, 1
- Méndez, R. H., Kudritzki, R. P., Herrero, A., Husfeld, D., & Groth, H. G. 1988, *A&A*, 190,
113
- Motch, C., Werner, K., & Pakull, M. W. 1993, *A&A*, 268, 561
- Napiwotzki, R. 1999, *A&A*, 350, 101

- Napiwotzki, R., Barstow, M. A., Fleming, T., Holweger, H., Jordan, S., & Werner, K. 1993, A&A, 278, 478
- Nelson, B., & Young, A. 1970, PASP, 82, 699
- Nousek, J. A., et al. 1986, ApJ, 309, 230
- O’Brien, M. S., Bond, H. E., & Sion, E. M. 2001, ApJ, 563, 971
- Patterson, J. 1994, PASP, 106, 209
- Perryman, M. A. C. et al. 1997, A&A, 323, L49
- Perryman, M. A. C. et al. 1998, A&A, 331, 81
- Raymond, J. C., & Smith, B. W. 1977, ApJS, 35, 419
- Reimers, D., & Cassatella, A. 1985, ApJ, 297, 275
- Ritter, H., & Kolb, U. 1998, A&AS, 129, 83
- Rucinski, S. M. 1984, A&A, 132, L9
- Saxton, R. D., Barstow, M. A., Turner, M. J. L., Williams, O. R., Stewart, G. C., & Kii, T. 1997, MNRAS, 289, 196
- Schmitt, J. H. M. M., Fleming, T. A., & Giampapa, M. S. 1995, ApJ, 450, 392
- Sion, E. M., & Downes, R. A. 1992, ApJ, 396, L79
- Sion, E. M., Holberg, J. B., Barstow, M. A., & Kidder, K. M. 1995, PASP, 107, 232
- Snowden, S. L., McCammon, D., Burrows, D. N., & Mendenhall, J. A. 1994, ApJ, 424, 714
- van Altena, W. F. 1969, AJ, 74, 2

- Vennes, S. 1990, ApJ, 361, L65
- Warner, B. 1972, MNRAS, 159, 95
- Wegner, G. 1979, MNRAS, 187, 17
- Wegner, G. 1981, AJ, 86, 264
- Werner, K. 1991, A&A, 251, 147
- Werner K., et al. 1997, in Reviews in Modern Astronomy 10, ed. R. E. Schielicke, Astronomische Gesellschaft, 219
- Werner, K., & Heber, U. 1992, in Atmospheres of Early Type Stars, ed. U. Heber & C. S. Jefferey (Berlin: Springer), 291
- Werner, K., Heber, U., & Fleming, T. 1994, A&A, 284, 907
- Werner, K., & Wolff, B . 1999, A&A, 347, L9
- White, N., Giommi, P., & Angelini, L. 2000, The WGA Catalogue of *ROSAT* Point Sources (WGACAT), available at <http://wgacat.gsfc.nasa.gov/wgacat/wgacat.html>
- Winget, D. E., Hansen, C. J., & van Horn, H. M. 1983, Nature, 303, 781

Figure Captions

Fig. 1.— WD 1910+047. Left: Broad-band Digitized Sky Survey image overlaid by X-ray contours at 10, 20, 50, 70, and 90% of the peak value of the X-ray source. The white dwarf is marked by two short lines near the center of the field of view. The X-ray source is clearly associated with a star $80''$ SE of the white dwarf. Right: *ROSAT* PSPC spectrum of the X-ray source. The X-ray contours and spectrum are extracted from the 20.6 ks observation rp500058a02.

Fig. 2.— Seventeen white dwarfs associated with hard X-ray emission. Left panels: Broad-band Digitized Sky Survey image overlaid by X-ray contours at 10, 20, 50, 70, and 90% of the peak value of the X-ray source. In some cases, the background is so high that the lower X-ray contours are absent. The white dwarf is at the center of each field of view. When multiple stars are projected in the vicinity of a white dwarf, we mark the white dwarf with two short lines. For white dwarfs with large proper motions, lines are drawn to show the proper motion from the optical epoch to the X-ray epoch. For WD 0736+053, the wavy line shows the proper and orbital motions of the white dwarf; for WD 1633+572, the arrow shows the motion of its common proper motion companion CM Dra. Right panels: *ROSAT* PSPC spectrum of the X-ray source. In cases where the spectrum is overwhelmed by soft X-ray emission, to show the hard X-ray emission, the spectrum is also plotted with open triangles after being multiplied by a constant factor indicated in the panel. The X-ray contours and spectra are extracted from *ROSAT* PSPC observations listed in Table 1.

Fig. 3.— KPD 0005+5106 (= WD 0005+511). Left: Broad-band Digitized Sky Survey image overlaid by X-ray contours at 10, 20, 50, 70, and 90% of the peak value of the X-ray source. The white dwarf is marked by two short lines near the center of the field of view. Two X-ray sources associated with two different stars are detected. Right: *ROSAT* PSPC spectrum of the X-ray source associated with the white dwarf KPD 0005+5106. This spectrum was carefully extracted to exclude the X-ray emission from the neighboring source. The X-ray contours and spectrum are extracted from the 5 ks observation rf200428n00 made with a boron filter. Hard X-ray emission at 1 keV is clearly detected.

Fig. 4.— Soft and hard X-ray images of eleven apparently single hot white dwarfs. The soft X-ray images (left panels) are extracted from PSPC observations in the 0.1–0.4 keV energy band, and the hard X-ray images (right panels) in the 0.6–2.4 keV energy band.

Table 1. White Dwarfs Coincident with WGACAT X-ray Sources

(1)	(2)	(3)	(4)	(5)	(6)	(7)	(8)	(9)	(10)
WD Number	Common Name	WD Type	WGACAT Number	ROSAT PSPC Obs. #	Exp. Time [ks]	Pos. Coin.	X-ray Counts 0.1-0.4 keV [cts]	Counts Reported in WGACAT 0.4-0.9 keV [cts]	Counts Reported in WGACAT 0.9-2.4 keV [cts]
0027-636	...	DA1	J0029.9-6324	400160	2.7	good	4081 ± 64	27 ± 5	0 ± 0
0037+312	GD 8	DA1	J0039.8+3132	201045	28.4	good	2248 ± 47	106 ± 10	65 ± 8
0048-294	FOCAP SGP2:31	DA	J0051.2-2910	700275	24.5	U1,2	46 ± 7	11 ± 3	24 ± 5
0050-332	GD 659	DA1	J0053.2-3300	200410	3.4	good	3787 ± 62	27 ± 5	3 ± 2
0116-231	GD 695	DA3	J0118.6-2254	100376	17.0	good	50 ± 7	5 ± 2	1 ± 1
0122-753J		DO	J0122.8-7521	300369	5.6	good	3130 ± 56	98 ± 10	8 ± 3
0131-163	GD 984	DA1+dM	J0134.4-1607	200485	0.9	good	633 ± 25	4 ± 2	0 ± 0
0136+251	PG 0136+251	DAp1	J0138.8+2523	200539	2.1	good	550 ± 24	5 ± 2	0 ± 0
0216-032	VZ Cet	DA+M2-7III	J0219.3-0258	201501	9.1	good	5 ± 2	18 ± 4	40 ± 6
0304+154	...	DC	J0307.0+1540	800104	7.7	U1,2	48 ± 7	11 ± 3	5 ± 2
0320-539	LB 1663	DA1.5	J0322.2-5345	800307	21.5	good	2534 ± 50	14 ± 3	1 ± 1
0333-350	...	DA	J0335.5-3449	600127	18.0	good	1480 ± 38	20 ± 4	5 ± 2
0339-451	...	DA	J0341.4-4500	900495	48.6	good	64 ± 8	22 ± 5	18 ± 4
0347+171	V471 Tau	DA2+K2V	J0350.4+1714	200107	31.8	good	6538 ± 81	688 ± 26	809 ± 28
0416-550	...	DA	J0417.1-5457	600456	17.8	good	254 ± 16	16 ± 4	11 ± 3
0425+168	EGGR 37	DA2	J0428.6+1658	200083	2.9	good	33 ± 6	3 ± 2	0 ± 0
0426+588	GJ 169.1B	DC+M4	J0431.1+5859	201114	3.5	good	22 ± 5	4 ± 2	4 ± 2
0429+176	HZ 9	DA2+dM4.5e	J0432.4+1744	200443	20.3	good	384 ± 20	180 ± 13	161 ± 13
0443-037J	RE J0443-034	DA	J0443.0-0346	200997	10.1	good	14710 ± 121	336 ± 18	42 ± 6
0446-789	...	DA3	J0443.6-7851	201073	8.3	good	74 ± 9	1 ± 1	1 ± 1
0518-105	RE J0521-102	DA2	J0521.3-1029	200830	5.3	good	370 ± 19	1 ± 1	0 ± 0
0531-022	RE J0534-021	DA2	J0534.3-0213	200932	8.0	good	284 ± 17	17 ± 4	6 ± 2
0548+000	GD 257	DA1	J0550.6+0005	200585	4.4	good	1404 ± 38	18 ± 4	0 ± 0
0558-756	...	DO	J0556.9-7540	201245	18.5	U2,3	10 ± 3	5 ± 2	13 ± 4

Table 1—Continued

(1)	(2)	(3)	(4)	(5)	(6)	(7)	(8)	(9)	(10)
WD Number	Common Name	WD Type	WGACAT Number	ROSAT PSPC Obs. #	Exp. Time [ks]	Pos. Coin.	X-ray Counts 0.1-0.4 keV [cts]	Counts Reported in 0.4-0.9 keV [cts]	WGACAT 0.9-2.4 keV [cts]
0651-020	GD 80	DA1	J0654.2-0209	201363	0.4	good	70 ± 8	1 ± 1	0 ± 0
0715-704J	RE J0715-705	DA1	J0715.2-7025	400321	2.8	good	5439 ± 74	27 ± 5	0 ± 0
0718-316	IN CMa	DAO+dM	J0720.7-3146	300338	3.2	good	411 ± 20	4 ± 2	2 ± 1
0734-143	...	DA	J0736.6-1428	500295	9.1	U3	5 ± 2	19 ± 4	23 ± 5
0736+053	Procyon B	DA+F5IV-V	J0739.3+0513	200437	3.8	good	11700 ± 110	874 ± 30	118 ± 11
0800-477J		DA	J0800.4-4745	400158	2.4	good	1333 ± 37	42 ± 6	0 ± 0
0805+654	PG 0805+654	DA1	J0809.6+6518	700258	8.4	U2	198 ± 14	67 ± 8	18 ± 4
0824+288	PG0824+289	DA+dC+M3	J0827.0+2844	201083	2.7	good	586 ± 24	5 ± 2	1 ± 1
0839-528	IC 2391 KR 1	DA3	J0841.1-5300	200501	22.9	U2,3	16 ± 4	14 ± 4	30 ± 6
0840+200	LB 1876	DA5	J0842.8+1951	200250	1.9	U2	11 ± 3	4 ± 2	10 ± 3
0841+033J	RE J0841+032	DA1	J0841.0+0320	201362	0.3	good	182 ± 13	1 ± 1	0 ± 0
0842+490	HD 74389B	DA+A2V	J0845.8+4852	200816	0.3	good	91 ± 10	3 ± 2	0 ± 0
0903+166	J0905.9+1624	700385	6.2	U2,3	21 ± 5	21 ± 5	12 ± 3
0904+511	PG 0904+511	DA1.5	J0907.7+5058	800474	9.6	good	524 ± 23	25 ± 5	26 ± 5
0916-197J	RE J0916-194	DA	J0916.9-1946	400162	2.9	good	1494 ± 39	19 ± 4	0 ± 0
0937+505	PG 0937+505	DA1	J0940.3+5021	200957	4.1	good	239 ± 16	0 ± 0	0 ± 0
0954+697	PG 0954+697	DA2.5	J0958.4+6928	600101	21.4	U4	174 ± 13	76 ± 9	38 ± 6
1010+064	PG 1010+065	DA1	J1013.4+0612	200540	6.8	good	204 ± 14	5 ± 2	2 ± 1
1032+534J	RE J1032+535	DA1	J1032.1+5330	900149	17.7	good	40710 ± 202	335 ± 18	81 ± 9
1040+451	PG 1040+451	DA1	J1043.5+4454	201020	14.7	good	1787 ± 42	66 ± 8	28 ± 5
1059+514J		DA	J1059.2+5124	400159	3.2	good	6582 ± 81	102 ± 10	0 ± 0
1109+244	PG 1109+244	DA1.5	J1112.6+2409	201365	0.2	good	46 ± 7	0 ± 0	0 ± 0
1134+300	GJ 433.1	DA2	J1137.0+2948	200091	33.9	good	327 ± 18	59 ± 8	51 ± 7
1144+004	...	DQZO1	J1146.5+0012	201242	5.8	good	149 ± 12	5 ± 2	3 ± 2

Table 1—Continued

(1)	(2)	(3)	(4)	(5)	(6)	(7)	(8)	(9)	(10)
WD	Common	WD	WGACAT	ROSAT	Exp.	Pos.	X-ray Counts Reported in WGACAT		
Number	Name	Type	Number	PSPC	Time	Coin.	0.1-0.4 keV	0.4-0.9 keV	0.9-2.4 keV
				Obs. #	[ks]		[cts]	[cts]	[cts]
1159-034	GW Vir	DQZO.4	J1201.7-0345	701202	13.6	good	779 ± 28	12 ± 4	13 ± 4
1213+528	EG UMa	DA4+dM2e	J1215.6+5230	200953	2.6	good	249 ± 16	68 ± 8	84 ± 9
1229+290	...	DC	J1231.7+2848	201163	1.8	U1,3	113 ± 11	44 ± 7	39 ± 6
1234+481	PG 1234+481	DA1	J1236.7+4755	200578	2.5	good	2127 ± 46	89 ± 9	0 ± 0
1254+223	GD 153	DA1	J1257.0+2201	132471	8.6	good	16673 ± 130	95 ± 10	0 ± 0
1255+258J	HD 112313	CSPN+G5III	J1255.5+2553	201514	18.8	good	90 ± 9	29 ± 5	39 ± 6
1314+293	HZ 43A	DA1+dM3.5e	J1316.3+2906	100308	21.5	good	1585270 ± 1260	7312 ± 86	120 ± 11
1317+453	GJ 2100	DA3.5	J1319.2+4505	900325	10.3	U1,2	34 ± 6	12 ± 4	14 ± 4 [†]
1325+581	EGGR 358	DA7	J1327.6+5755	600458	18.1	U2,4	247 ± 16	35 ± 6	44 ± 7 [†]
1333+510	PG 1333+510	DA	J1335.2+5049	800047	16.4	good	447 ± 21	51 ± 7	47 ± 7 [†]
1403-077	PG 1403-077	DA1	J1406.0-0758	200528	4.8	good	345 ± 19	9 ± 3	1 ± 1
1446+634J	...	DA1	J1446.0+6329	700975	4.2	good	467 ± 22	5 ± 2	2 ± 1
1501+664	RE J1502+661	DZ1	J1502.1+6612	170001	43.2	good	357416 ± 600	1689 ± 41	12 ± 4
1522+662	...	DO	J1522.9+6604	201240	4.7	good	742 ± 27	13 ± 4	1 ± 1
1620-391	EGGR 274	DA2	J1623.5-3913	200588	1.9	good	634 ± 25	2 ± 1	2 ± 1
1631+781	1ES 1631+78.1	DA1+dM4e	J1629.1+7804	170154	37.5	good	125636 ± 350	1355 ± 37	350 ± 19
1633+572	GJ 630.1B	DQ8+dM4e	J1634.3+5709	200721	47.5	good	2397 ± 49	1249 ± 35	1038 ± 32
1634-573	HD 149499B	DOZ1+K2Ve	J1638.5-5728	200773	1.4	good	240 ± 16	145 ± 12	146 ± 12
1636+351	PG 1636+351	DA1.5	J1638.4+3500	201082	4.2	good	909 ± 30	9 ± 3	0 ± 0
1641+387	GD 357	DA3	J1643.1+3840	201538	5.5	U1	26 ± 5	10 ± 3	13 ± 4
1650+406J	RE J1650+403	DA1	J1650.3+4037	201080	2.2	good	55 ± 7	1 ± 1	0 ± 0
1657+343	PG 1657+343	DA2	J1658.8+3418	201079	6.4	good	591 ± 24	7 ± 3	0 ± 0
1658+440	PG 1658+440	DAp1	J1659.8+4400	201078	6.7	good	503 ± 22	7 ± 3	1 ± 1
1659+442	PG 1659+442	DA	J1700.6+4410	201078	6.7	U1,2	22 ± 5	7 ± 3	7 ± 3

Table 1—Continued

(1)	(2)	(3)	(4)	(5)	(6)	(7)	(8)	(9)	(10)
WD Number	Common Name	WD Type	WGACAT Number	ROSAT PSPC Obs. #	Exp. Time [ks]	Pos. Coin.	X-ray Counts 0.1-0.4 keV [cts]	Counts Reported in 0.4-0.9 keV [cts]	WGACAT 0.9-2.4 keV [cts]
1802+213	GD 372	DA4	J1804.4+2120	200940	13.7	U2,3	35 ± 6	21 ± 5	14 ± 4
1821+643	DS Dra	DOZ.4	J1821.8+6422	700948	2.0	good	135 ± 12	9 ± 3	20 ± 5
1844-654	...	DA	J1848.9-6525	200941	16.0	good	757 ± 28	126 ± 11	64 ± 8
1906-600	...	DC	J1910.8-5958	300047	5.2	U3	7 ± 3	20 ± 5	41 ± 6
1910+047	...	DA2	J1912.5+0452	400271	2.8	U4	20 ± 45	10 ± 3	27 ± 5
1944-421	V3885 Sgr	CV	J1947.6-4200	300232	10.4	good	345 ± 19	448 ± 21	699 ± 26
1957+225	...	DAO	J1959.6+2243	900016	5.9	good	828 ± 29	5 ± 2	0 ± 0
2013+400J	RE J2013+400	DAO	J2013.1+4002	400157	3.0	good	1166 ± 34	17 ± 4	9 ± 3
2014-575	RE J2018-572	DA2	J2018.8-5721	200580	4.1	good	148 ± 12	3 ± 2	0 ± 0
2020-425	UVE J2024-42.4	DA	J2023.9-4224	200488	0.9	good	71 ± 8	2 ± 1	0 ± 0
2028+390	GD 391	DA2	J2029.9+3913	200412	2.2	good	46 ± 7	0 ± 0	0 ± 0
2032+248	HD 340611	DA2.5	J2034.3+2504	200087	9.9	good	100 ± 10	2 ± 1	5 ± 2
2034-275J		DA	J2034.9-2734	201236	5.0	good	574 ± 24	4 ± 2	2 ± 1
2052+466J		DO	J2052.6+4639	200114	3.5	U3	801 ± 28	118 ± 11	27 ± 5
2056+033	PG 2056+033	DA1	J2058.7+0332	200955	5.6	good	37 ± 6	2 ± 1	1 ± 1
2111+498	GD 394	DA1.5	J2112.7+5006	200427	0.4	good	207 ± 14	1 ± 1	0 ± 0
2117+342J	V2027 Cyg	DO	J2117.1+3412	201512	26.6	good	6588 ± 81	194 ± 14	66 ± 8
2153-419	RE J2156-414	DA	J2156.5-4142	200487	0.7	good	397 ± 20	2 ± 1	0 ± 0
2154-512	GJ 841B	DQ7+dM3-5e	J2157.7-5059	600146	5.1	good	1851 ± 43	606 ± 25	706 ± 27
2309+105	GD 246	DA1	J2312.3+1047	100578	10.3	good	36832 ± 190	141 ± 13	3 ± 2
2321-549	RE J2324-544	DA	J2324.5-5441	400166	4.1	good	1964 ± 44	20 ± 5	1 ± 1
2357+296	PG 2357+296	DA1	J0000.1+2956	200535	3.8	good	36 ± 6	2 ± 1	1 ± 1

Table 2. White Dwarfs with Hard X-ray Emission

WD Number	Spectral Type	Parallax ^a (mas)	$\log a^b$ (AU)	kT^c (keV)	$\log L_X^d$ (ergs s ⁻¹)
0216–032	DA+M2-7III	7.79±1.07	2.04:	0.5	29.9
0339–451	DA
0347+171	DA2+K2V	21.37±1.62	–1.81	0.8	29.8
0429+176	DA2+dM4.5e	21.58 ^e	–1.91	0.6	28.6
0736+053	DA+F5IV-V	285.93±0.88	1.20	0.2	27.3
1134+300	DA2+(AGN)	65.28±3.61
1159–034	DQZO.4
1213+528	DA4+dM2e	33.4 ±4.1 ^f	–1.89	0.8	28.8
1234+481	DA1	6.3 ^g
1255+258J	CSPN+G5III	4.70±0.75 ^h	>0.	0.7	29.3
1314+293	DA1+dM3.5e	31.26±8.33	≥1.85	0.6	28.0
1333+510	DA
1631+781	DA1+dM4e	19. ^g	>0.	0.8	28.7
1633+572	DQ8+2(dM3-4e)	68.4 ±3.3 ⁱ	≥2.58	0.4	28.0
1634–573	DOZ1+K2Ve	26.94±1.88 ^j	≥1.69	0.7	29.3
1944–421	CV	9.11±1.95	–2.09	1.2	30.3
2154–512	DQ7+2(dM3-5e)	61.63±2.67 ^k	≥2.66	0.8	29.0

^a*Hipparcos* trigonometric parallaxes (Perryman et al. 1997) unless otherwise noted.

^bThese values are derived from visual orbits, apparent separations, or orbital periods cited in §3.1, supplemented by parallaxes tabulated here and, for short-period systems, mass estimates from Ritter & Kolb (1998). For V471 Tau = WD 0347+171, masses were adopted from O’Brien, Bond, & Sion (2001).

^cFor $T = 10^6$ K, $kT = 0.086$ keV.

^dIn the 0.5 – 2.4 keV energy band.

^eAssumes membership in the Hyades (van Altena 1969) with distance from Perryman et al. (1998).

^fTrigonometric parallax from Dahn et al. (1982).

^gParallax deduced from EUV/IR photometric models of Green, Ali, & Napiwotzki (2000).

^hTrigonometric parallax from Harris et al. (1997).

ⁱTrigonometric parallax from Harrington & Dahn (1980); weighted mean

Table 3. Multi-band Photometry of White Dwarfs with Hard X-rays

WD Number	Spectral Type	V (mag)	J (mag)	H (mag)	K (mag)	2MASS ^a Source
0005+511	DO	13.32	13.93	14.13	14.18	J0008181+512316
0216–032	DA+M2-7III	11.32 ^b	–1.06	–1.89	–2.44	J2192081–025841 ^c
0429+176	DA2+dM4.5e	13.93	10.76	10.12	9.93	J0432237+174502
1134+300	DA2+(AGN)	12.50	12.95	13.04	13.13	^d
1159–034	DQZO.4	14.87 ^e	15.58	15.87	15.78	J1201459–034540
1234+481	DA1	14.42	14.99	15.07	15.12	J1236451+475522
1631+781	DA1+dM4e	13 ^f	11.00	10.28	10.15	J1629102+780439
1633+572	DQ8 +	14.99	14.09	14.08	14.07	J1634216+571008
	2(dM3-4e)	12.87 ^g	8.50	8.04	7.77	J1634204+570943
2226–210	DAO	13.54	14.35	14.50	14.62	J2229385–205013

^aThe Two Micron All Sky Survey (2MASS) is a joint project of the University of Massachusetts and the Infrared Processing and Analysis Center/California Institute of Technology.

^bHubble Space Telescope $F5550M$ magnitude, equivalent to Strömgen y magnitude, of the white dwarf alone (Karovska et al. 1997).

^cSaturated in 2MASS survey. J , H , and K from Catchpole et al. (1979). Variable in all bandpasses.

^d V – Massey & Gronwall (1990); J , H , and K – Hawarden et al. (2001).

^e y magnitude.

^f B magnitude.

^gOut-of-eclipse maximum.

Table 4. Properties of the Hottest Apparently Single White Dwarfs

WD Number	Spectral Type ^a	T_{eff} ^b [K]	V ^a [Mag]	X-Ray ^c	Exp. Time ^d [ks]
WD 0005+511	DO	120,000	13.32	S, H	5.0
WD 0044–121	PG 1159	150,000	11.84	S	11.4
WD 0122–753J	DO	180,000	15.4	S, H?	5.6
WD 0726+133	PG 1159	140,000 ^e	15.99	ND	2.8
WD 1144+004	DQZO1	150,000	15.10	S	5.8
WD 1159–034	DQZO.4	140,000	14.84	S, H	13.6
WD 1501+664	DZ1	170,000	15.9	S	43.2
WD 1522+662	DO	140,000	16.4 ^f	S	4.7
WD 1821+643	DOZ.4	140,000 ^g	15.04	S	3.1
WD 1957+225	DAO	108,600	14.2	S	19.9
WD 2117+342J	DO	170,000	13.16	S	26.6
WD 2226–210	DAO	103,600	13.4	S, H	4.9
WD 2333+301	DOZ.3	150,000 ^e	16.13	ND	4.2

^aVisual magnitude from McCook & Sion (1999), unless noted otherwise.

^bStellar effective temperature from Napiwotzki (1999), unless noted otherwise.

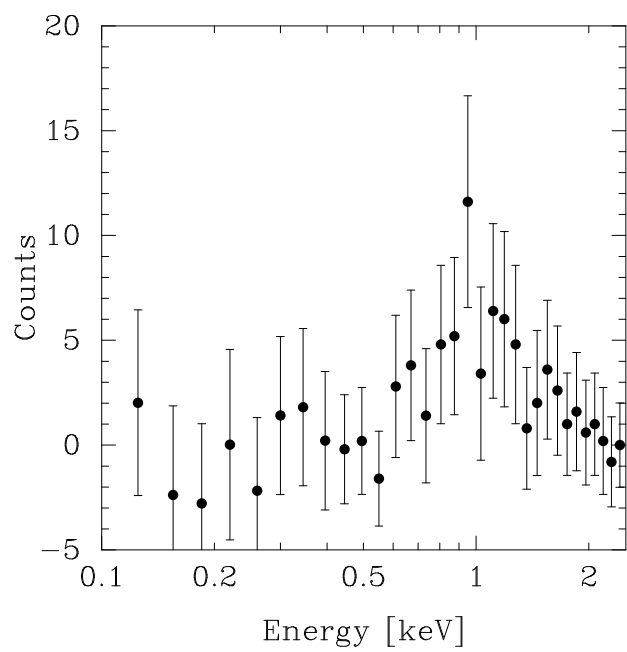
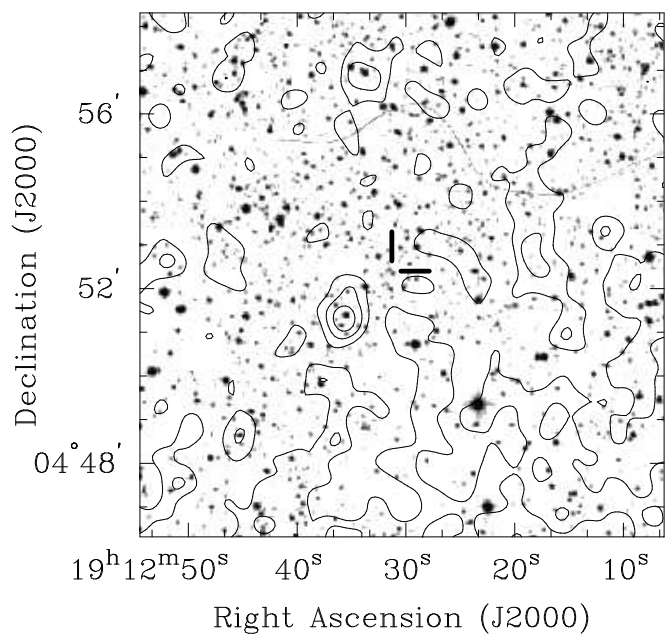
^cX-ray emission detected by *ROSAT* PSPC observations. ND: not detected; S: detected in the 0.1–0.5 keV band; H: detected in the 0.6–2.4 keV band.

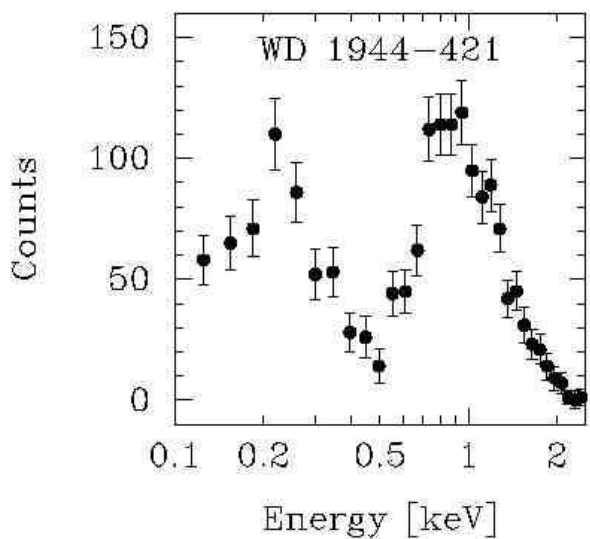
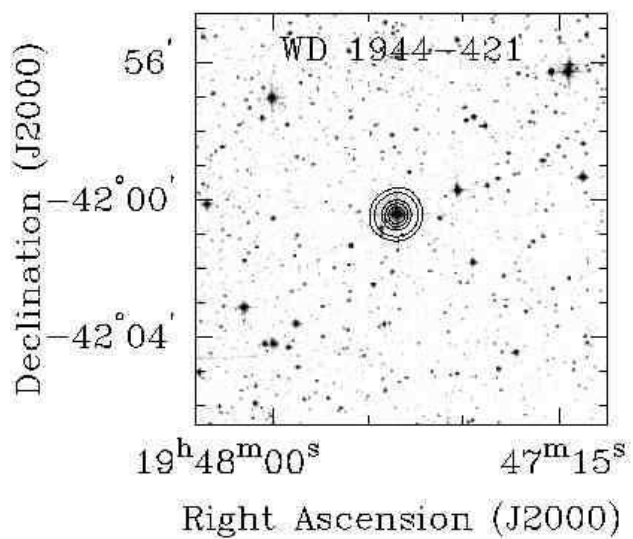
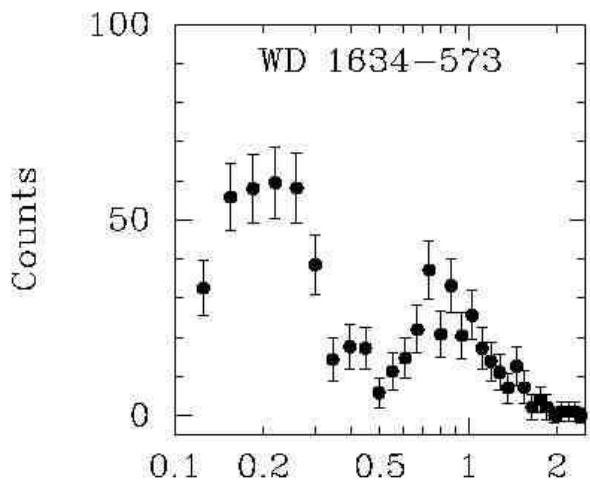
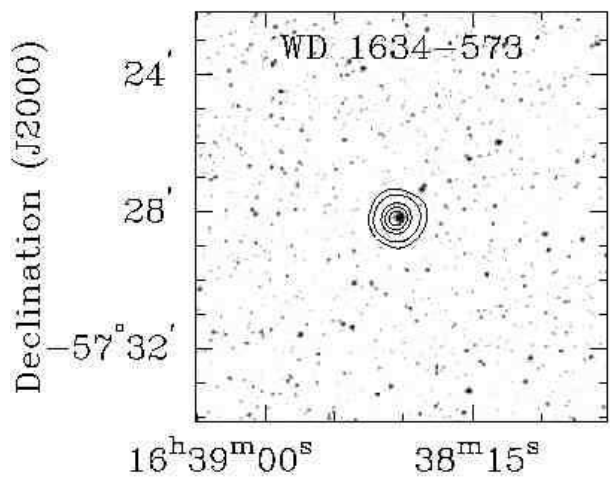
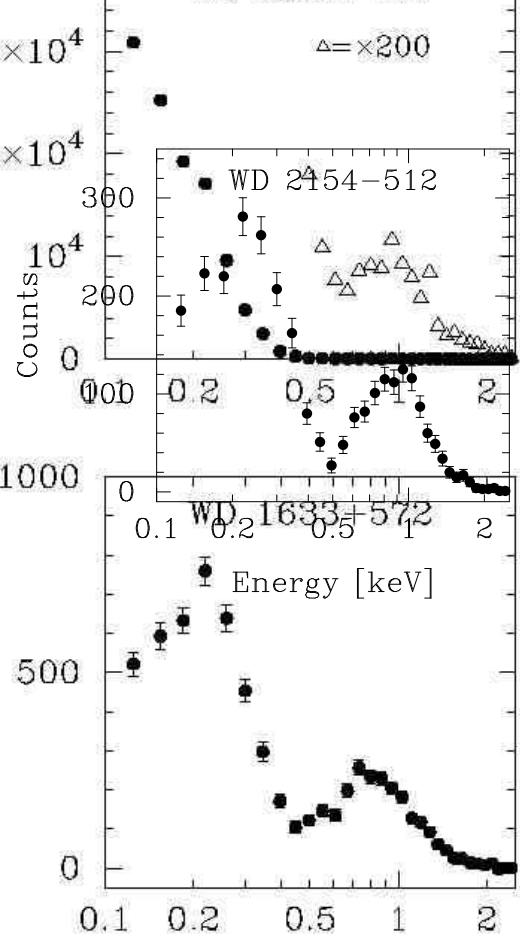
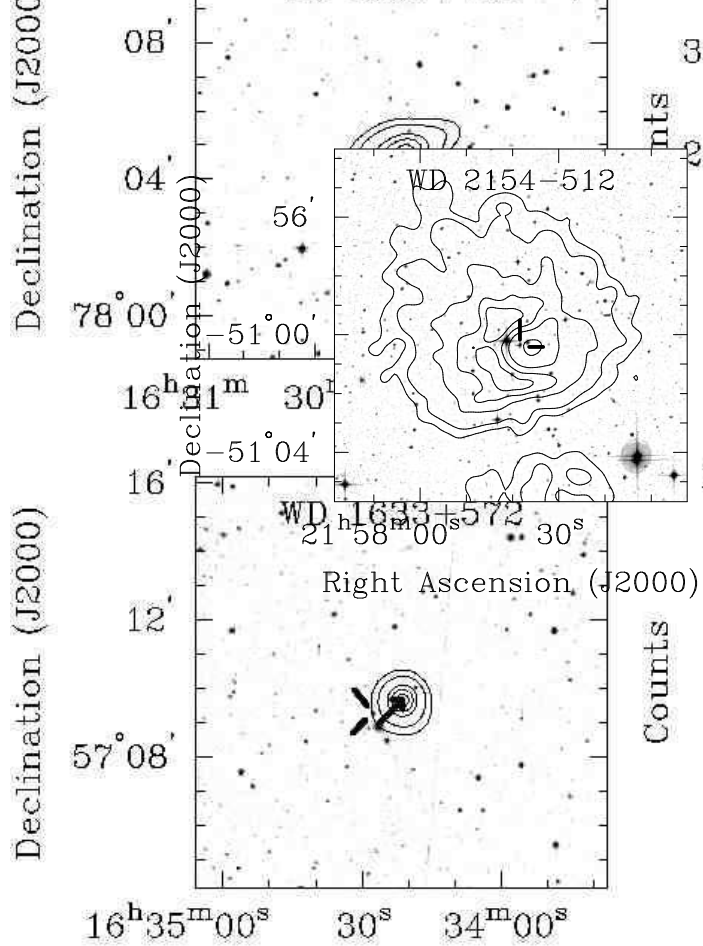
^dExposure time of available *ROSAT* PSPC observation.

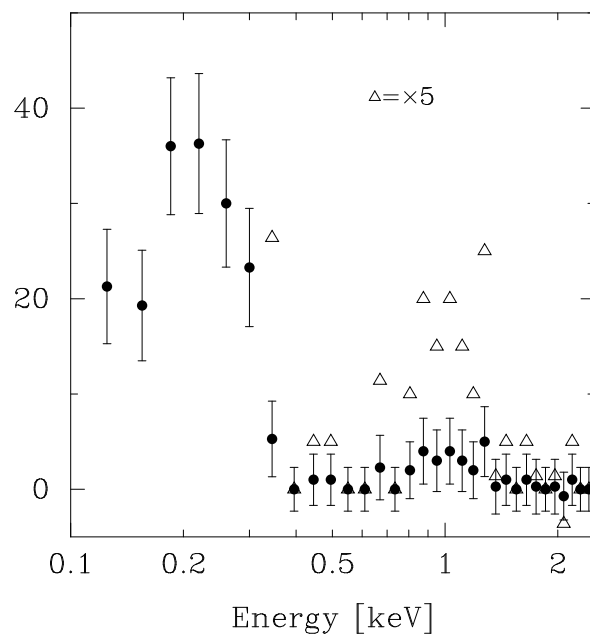
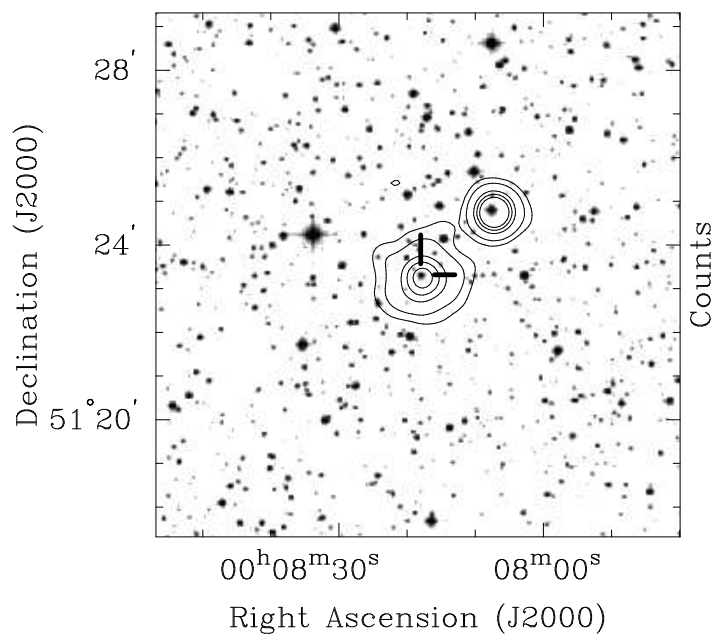
^eFrom Werner et al. (1997).

^f B magnitude from McCook & Sion (1999).

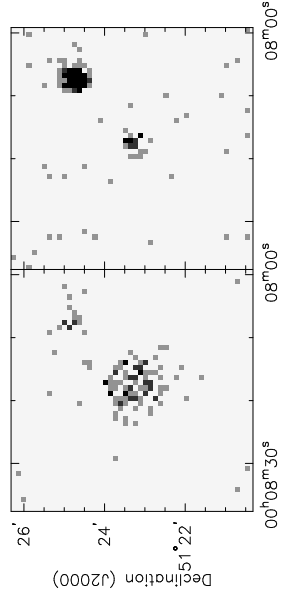
^gFrom Koesterke, Dreizler, & Rauch (1998).



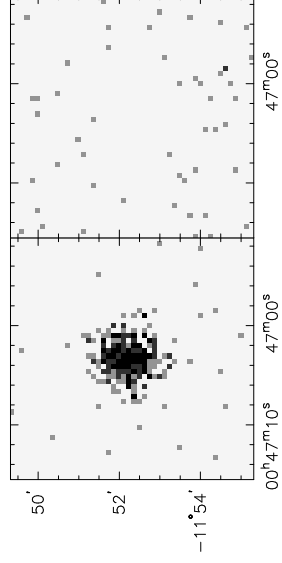




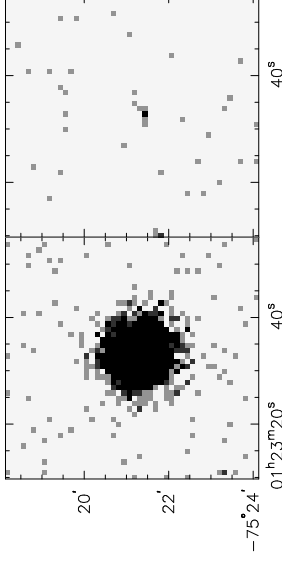
WD 0005+511



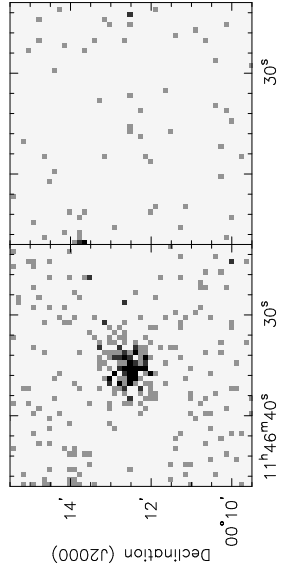
WD 0044-121



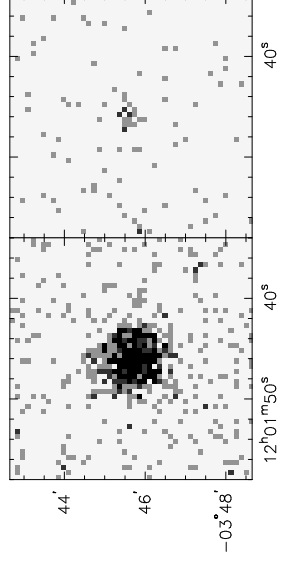
WD 0122-753J



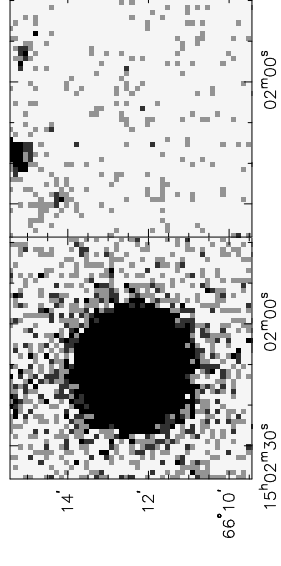
WD 1144+004



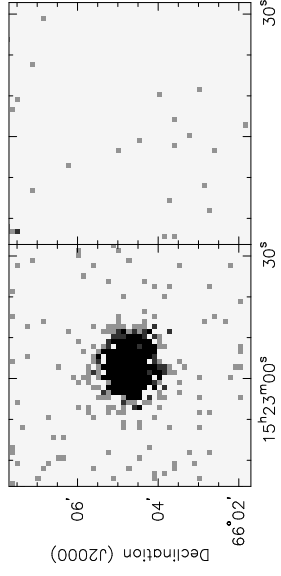
WD 1159-034



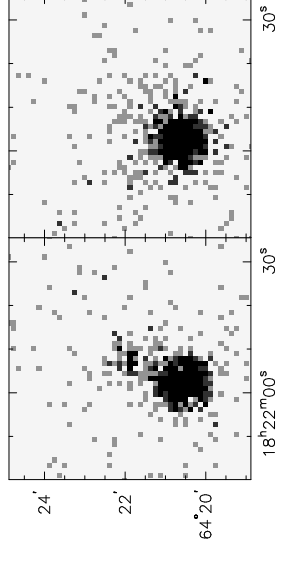
WD 1501+664



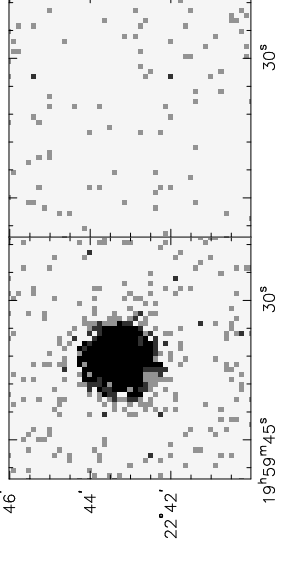
WD 1522+662



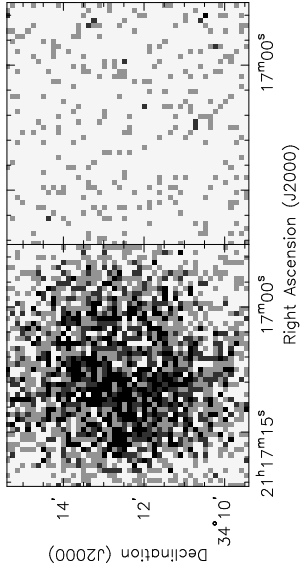
WD 1821+643



WD 1957+225



WD 2117+342J



WD 2226-210

